



Kinetic modeling of glycerol acetylation catalyzed by styrene–divinylbenzene and styrene-trimethylolpropane triacrylate sulfonated resins

William M. Godoy¹ · Juliana A. Carpegiani¹ · Félix M. Pereira¹ · Daniela H. P. Guimarães¹ · Leandro G. Aguiar¹

Received: 19 October 2021 / Accepted: 15 December 2021
© Akadémiai Kiadó, Budapest, Hungary 2021

Abstract

The present work reports a kinetic comparison between two resins made with different cross-linkers, Amberlyst 36 and PS-TMPTA. The latter was synthesized in this study. Both resins were used as catalysts in glycerol acetylation in a batch reactor at 80 and 90 °C, with 5 and 10 g L⁻¹ of catalyst concentration under a molar ratio 4:1 of acetic acid/glycerol. The synthesized resin (PS-TMPTA) presented low ion exchange capacity (1.5 mmol g⁻¹) compared to the commercial resin (Amberlyst 36, 5.45 mmol g⁻¹), but both presented similar efficiency in catalysis, probably due to the difference in cross-linking densities. The experimental results explain the resins' behavior and properties in detail (ion exchange capacities, swelling index and catalytic efficiency) and the kinetic models were compared utilizing the difference between the corrected Akaike Information Criterion (ΔAIC_c), Standard Deviation (s) and P-value (student t distribution). According to the results, the irreversible first order model had the best fit of the two models for the experimental conditions studied for this work.

Keywords Acetylation · Resin · Catalysis · Modeling

Introduction

Biodiesel is gradually replacing fossil fuels, especially in transportation, and it has the ambitious environmental objective of reducing the gaseous emissions of combustion that are harmful to the atmosphere [1, 2]. Because of the constant increase

✉ Leandro G. Aguiar
leandroaguiar@usp.br

¹ Department of Chemical Engineering, Engineering School of Lorena, University of São Paulo, Lorena, SP 12602-810, Brazil

in production of this type of fuel, there has been an accumulation of raw glycerol (which is a byproduct of this process) since industrial demand is not high enough to absorb this excessive glycerol production [3, 4].

There are currently studies on refining glycerol that are not only focused on producing glycerol-derived products, but also on identifying them. There are routes to generate high added value products from glycerol, such as etherification and esterification. This last route uses acetylation in its process, especially with acetic acid. These processes are able to produce ethers and esters of commercial interest [1, 3–7].

Even though acetylation is an autocatalytic reaction, techniques that assist the reaction still have to be used. The use of ion exchange resins could be highlighted in this regard (as they are a way to increase the yield of the desired product, i.e., a way to favor the kinetic rate without affecting the chemical balance) [8–10].

Current studies project that Amberlyst 36 (crosslinked with divinylbenzene) and other resins could be applied in the catalysis of glycerol with acetic acid. On the other hand, resins crosslinked with other monomers, such as triethylene glycol dimethacrylate (TEGDMA), ethylene glycol dimethacrylate (EGDMA) and trimethylolpropane triacrylate (TMPTA) have shown a distinct efficiency in the referred reaction [11–13]. Furthermore, some studies related to catalytic decay have shown that these resins can be reutilized without losing their catalytic properties [4, 9].

Kinetic models are of utmost importance to describe and improve processes [14]. In this regard, common approaches are used to describe the glycerol acetylation, such as: (a) homogeneous and heterogeneous reversible second order models [1, 8, 15]; and (b) homogeneous irreversible first order models [7].

Despite the literature using first and second order models, there are few studies involving comparisons between them and other models (such as irreversible second order and reversible first order) employing statistical techniques. This approach, which uses such techniques, is more precise in comparing the efficiency of the various catalysts and models. The current work assessed kinetic models for the esterification reaction of glycerol with acetic acid catalyzed by sulfonated resins. The models were compared with original experimental data and those from the literature. In terms of catalytic efficiency, the Amberlyst 36 resin was compared with the resin synthesized in this study, which was cross-linked with TMPTA.

Experimental method

Suspension copolymerization

The copolymerization method used is described in the literature [9, 11]. The present reaction between styrene and TMPTA was conducted in a 1 L jacketed glass reactor at 80 °C with stirring at 350 rpm. The suspension copolymerization was fed as a mixture of organic and aqueous phases. The organic phase was composed of 1 mol % of initiator (benzoyl peroxide), 0.4 of monomer fraction (styrene), 0.1 fraction of trimethylolpropane triacrylate (TMPTA) in the monomer mixture, 0.5 fraction of

toluene in the toluene + heptane mixture, and the aqueous phase was prepared with polyvinyl alcohol (0.1%). The copolymerization reaction was conducted in 6 h.

Sulfonation reaction

The dried copolymers (approximately 10 g) were kept in contact with sulfuric acid (140 mL) at 57.5 °C for 1 h under stirring at 175 rpm. Subsequently, the mixture (resins and sulfuric acid) was diluted in distilled water at 25 °C and the sulfonate resin was filtered. The experimental conditions were based on previous studies [12, 13, 16].

Ion exchange capacity analysis

This procedure was carried out for both catalysts (Amberlyst 36 and PS-TMPTA) and can be found in literature [17–19]. Five grams of dried resin were immersed in nitric acid (1 mol L⁻¹, 8 mL) for 4 h. The particles were filtered, dried to constant mass, and put in contact with sodium hydroxide (0.1 mol L⁻¹, 24 mL) for 24 h. Subsequently, the solution was titrated with hydrochloric acid (0.1 mol L⁻¹), and the ion exchange capacity (IEC) was determined according to Eq. (1).

$$\text{IEC} = C_{\text{HCl}} \frac{V_{\text{NaOH}} - V_{\text{t}}}{w_{\text{d}}} \quad (1)$$

here IEC is the ion exchange capacity (mmol g⁻¹), C_{HCl} is the hydrochloric acid concentration (mmol mL⁻¹), V_{NaOH} is the volume of sodium hydroxide solution (mL), V_{t} is the titrated volume of hydrochloric acid (mL) and w_{d} is the dried catalyst mass (g).

Swelling index

The swelling index was calculated by following a method from literature [1]. After the glycerol acetylation, the catalyst was withdrawn and its mass was measured, still moist, and then dried until constant mass. The swelling index (Sw) was calculated by dividing the moist mass of catalyst (w_{m}) by the dry mass of catalyst (w_{d}), according to Eq. (2).

$$\text{Sw} = \frac{w_{\text{m}}}{w_{\text{d}}} \quad (2)$$

Catalytic efficiency

The catalytic efficiency was calculated as described in the literature [9]. This procedure consists in dividing the number of mols of a given reagent consumed in the reaction by the amount of catalytic sites in the medium, in order to assess the

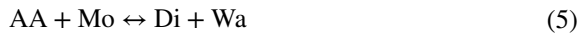
catalytic sites efficiency of the resins, since both present the same catalytic sites (SO_3H). Equation (3) shows how to make this calculation.

$$Ef = \frac{N_c}{IEC * N_{cat}} \quad (3)$$

here Ef is the catalytic efficiency, N_c is the number of mols of glycerol (mmol) consumed at the end of the reaction (6 h), IEC is the ion exchange capacity (mmol g^{-1}) and N_{cat} is the amount of catalyst fed to the reactor (g). In this work, the reaction time was 6 h.

Kinetic modelling

The esterification of glycerol with acetic acid consists of three reactions that form four products: monoacetin, diacetin, triacetin and water, represented by Eqs. (4–6) [11, 20]:



here AA is acetic acid, Gl is glycerol, Mo is monoacetin, Di is diacetin, Tr is triacetin and Wa is water. The literature states that when this reaction is catalyzed by polymeric resins, whose particles have high swelling, the diffusive effects can be disregarded [1, 7, 9, 15]. At first, four kinetics were considered: reversible and irreversible second and first order models. The relevance of all kinetic parameters of the models was verified. Both reversible models (the first and the second order) were rejected since their reversible kinetic parameters did not affect the modeling results.

The irreversible second order model was therefore one of the two models studied here, (Eqs. 7–9) [21]:

$$r_{gl1} = -k_1 C_{aa} C_{gl} \quad (7)$$

$$r_{mo2} = -k_2 C_{aa} C_{mo} \quad (8)$$

$$r_{di3} = -k_3 C_{aa} C_{di} \quad (9)$$

here r was the reaction rate of the formation of the limiting reactant and C_i was the concentration of the substance i (in mol m^{-3}). The differential equations per substances are represented by Eqs. (10–14), where t is the time (in s).

$$\frac{dC_{gl}}{dt} = -k_1 C_{aa} C_{gl} \quad (10)$$

$$\frac{dC_{mo}}{dt} = -k_2 C_{aa} C_{mo} + k_1 C_{aa} C_{gl} \quad (11)$$

$$\frac{dC_{di}}{dt} = -k_3 C_{aa} C_{di} + k_2 C_{aa} C_{mo} \quad (12)$$

$$\frac{dC_{tr}}{dt} = k_3 C_{aa} C_{di} \quad (13)$$

$$\frac{dC_{aa}}{dt} = -k_1 C_{aa} C_{gl} - k_2 C_{aa} C_{mo} - k_3 C_{aa} C_{di} \quad (14)$$

The second model used was the irreversible first order model, based on equations in the literature [7, 21] (Eqs. 15–19):

$$\frac{dC_{gl}}{dt} = -k_1 C_{gl} \quad (15)$$

$$\frac{dC_{mo}}{dt} = -k_2 C_{mo} + k_1 C_{gl} \quad (16)$$

$$\frac{dC_{di}}{dt} = -k_3 C_{di} + k_2 C_{mo} \quad (17)$$

$$\frac{dC_{tr}}{dt} = k_3 C_{di} \quad (18)$$

$$\frac{dC_{aa}}{dt} = -k_1 C_{gl} - k_2 C_{mo} - k_3 C_{di} \quad (19)$$

For water, Eq. (20) was written by molar balance:

$$C_{wa} = C_m + 2C_{di} + 3C_{tr} \quad (20)$$

The resins' efficiencies were compared by using the regression results with the glycerol consumption. The experimental conditions are described in Table 1.

The systems of differential equations [Eqs. (10–14) and Eqs. (15–19)] were numerically integrated with algorithms from the Adams method and adjusted with a nonlinear Levenberg Marquardt method [22] with a weight of the inverse of maximum concentration of the substance i , $C_{i\max}^{-1}$.

The simulation program Wolfram Mathematica® 12.3 Student Edition was used and provided results on the kinetic constants, the difference between the Corrected Akaike Information Criteria (ΔAIC_c), Standard Deviation(s) and P-value (student t distribution). For experiments that had more than two models, the smaller difference between AIC_c was chosen as the most suitable and this was described by Eq. (21).

Table 1 Glycerol acetylation experimental conditions

Run	Resin	Acetic acid/glycerol molar ratio	Resin concentration (g L ⁻¹)	Temperature (°C)
B080		4:1	0	80
B090				90
T580	PSTMPTA		5	80
T590				90
T1080			10	80
T1090				90
A580	Amberlyst 36		5	80
A590				90
A1080			10	80
A1090				90

$$\Delta AIC_c = AIC_{c1} - AIC_{c2} \quad (21)$$

here AIC_{c1} refers to AIC_c for the irreversible first order model and AIC_{c2} refers to AIC_c for the irreversible second order model. Models that presented kinetic parameters with a P-value higher than 5% [23] were also disregarded for the next steps.

Results and discussion

The ion exchange capacity (IEC), swelling index and catalytic efficiency (Ef) results for each resin are shown in Table 2.

When analyzing the results obtained with the catalysts PS-TMPTA and Amberlyst 36 and their properties, the difference in the content of the catalytic sites can be observed: while Amberlyst 36 had 5.45 mmol g⁻¹, the synthesized resin had 1.5 mmol g⁻¹, which is lower when compared to commercial resins, as shown in Table 2. Although this difference in ion exchange capacity, at 180 min both resins reaching greater glycerol conversions, being 90% from Amberlyst 36 and 62% to synthesized resin, as shown the Fig. S1.

Table 2 Comparison between properties of commercials and synthesized resins. The consumed mols of glycerol was measured at the end of the reaction

Resins	Temperature (°C)	IEC (mmol g ⁻¹)	Swelling index	Ef	References
Amberlyst 36	90	5.45	1.725	64.762	Present work
PS-TMPTA	90	1.50	7	230.122	Present work
Amberlyst 15	–	5.23	–	–	[24]
Amberlyst 35	–	5.20	–	–	[25]

Table 3 Kinetic parameters k_j and their Standard Deviation for the irreversible first order model

Run	k_1	s	k_2	s	k_3	s
B80	2.07	± 0.15	0.55	± 0.18	0.00	± 0.00
B90	3.39	± 0.17	1.16	± 0.20	0.00	± 0.00
T580	2.36	± 0.22	0.54	± 0.25	0.00	± 0.00
T590	4.55	± 0.39	1.85	± 0.38	0.00	± 0.00
T1080	3.47	± 0.40	1.30	± 0.46	0.00	± 0.00
T1090	7.86	± 0.34	4.74	± 0.34	0.77	± 0.28
A580	9.85	± 0.75	4.26	± 0.48	0.95	± 0.43
A590	18.78	± 1.94	5.48	± 0.64	1.11	± 0.42
A1080	20.34	± 1.67	5.71	± 0.44	1.10	± 0.29
A1090	23.49	± 1.79	6.78	± 0.46	1.22	± 0.26

The parameters were multiplied by 10^5s^{-1}

Table 4 Kinetic parameters k_j and their Standard Deviation for the irreversible second order model

Run	k_1	s	k_2	s	k_3	s
B080	1.82	± 0.36	0.48	± 0.39	0.00	± 0.00
B090	3.18	± 0.39	1.10	± 0.45	0.00	± 0.00
T580	1.87	± 0.48	0.42	± 0.50	0.00	± 0.00
T590	3.76	± 0.82	1.59	± 0.80	0.00	± 0.00
T1080	2.69	± 0.84	1.05	± 0.96	0.00	± 0.00
T1090	7.02	± 0.77	4.66	± 0.92	0.71	± 0.74
A580	10.36	± 1.41	5.25	± 1.14	1.18	± 0.89
A590	17.24	± 2.82	6.52	± 1.59	1.38	± 1.00
A1080	21.66	± 2.56	7.97	± 1.16	1.61	± 0.75
A1090	23.87	± 2.01	10.18	± 0.98	1.94	± 0.57

The parameters were multiplied by $10^9 \text{m}^3 \text{mol}^{-1} \text{s}^{-1}$

Despite the difference in IECs, both resins reached similar conversion profiles. This behavior suggests an effect of the cross-linker, which may provide better accessibility to catalytic sites, since both resins are composed of the same catalytic sites (sulfonic groups). In order to adequately estimate the catalytic activity of each resin, the catalytic efficiency were calculated, which was 230.122 for the synthesized resin (PS-TMPTA), more than three times greater in comparison with the commercial resin (64.762). The hypothesis of better accessibility to catalytic sites, provided by the cross-linker, is corroborated through the calculated swelling index, as shown in Table 2, which was 7 for the synthesized resin, a higher value than the commercial resin (1.725).

For experiments with no resin (Blank) and PS-TMPTA (except for experiment T1090), the parameter k_3 from Eqs. (12) and (17) was set to 0 in Tables 3, 4 and Table S1 since they had no formation of triacetin.

For the second step, which is presented in Table S2 (the ΔAIC_c), only 4 of 10 runs fitted in irreversible first order model (B090, T1080, T1090 and A590), while 6 fitted better for the irreversible second order model (B080, T580, T590, A580, A1080 and A1090).

For the third step, the P-value [Table S1], the parameter k_2 was insignificant for B080, T580, T590 and T1080 (in the irreversible second order model), while the same applied to experiments T1090, A580 and A590 for the parameter k_3 . Therefore, the ΔAIC_c results for B080, T580, T590 and A580 fitted in the irreversible second order model can be disregarded and only experiments A1080 and A1090 had a good fit for this model alone.

For the last step, the Standard Deviation for the kinetic parameters of the irreversible first order model is shown in Table 3. Meanwhile, Table 4 shows the results for the irreversible second order model.

Table 4 shows how some deviations were higher than the parameter value itself for the better fitted experiments of the irreversible first order model, especially for the parameters k_2 (T580) and k_3 (T1090).

For the same reaction, although catalyzed by Amberlyst 15 with a slurry reactor, the literature provides the approximate values for k_1 , k_2 and k_3 of: 1.68×10^{-4} , 7.52×10^{-5} , $8.84 \times 10^{-5} \text{ s}^{-1}$ at $80 \text{ }^\circ\text{C}$ and 2.88×10^{-4} , 1.01×10^{-4} and $1.01 \times 10^{-4} \text{ s}^{-1}$ at $90 \text{ }^\circ\text{C}$ [7]. Even though these literature data were obtained from experimental conditions that are different from these of the present study, it is worth noting that both Amberlyst 15 and the PS-TMPTA have sulfonic groups as catalytic sites, which are likely to lead to similar catalytic mechanisms. Fig. 1 shows some differences between substance curves when the temperature was changed from 80 to $90 \text{ }^\circ\text{C}$ for the resin PS-TMPTA, specially from (c) to (d), where a higher consumption of both reagents (acetic acid and glycerol) is observed and, consequently, higher formation of monoacetin, diacetin and the appearance of triacetin. It can be verified that increasing $10 \text{ }^\circ\text{C}$ to the temperature and adding 5 g L^{-1} of catalyst loading have contributed for speeding up the whole process, as expected. From the modeling standpoint, clear differences are observed in the concentration profiles when temperature is increased (e.g., Monoacetin in graphs 1a and 1b). On the other hand, when catalyst concentration is increased, the shift in model curves are less pronounced, however, the formation of triacetin is observed when comparing 1b and 1d.

It is important to point out that all experimental concentrations were determined by gas chromatography, including the first point ($t=0 \text{ s}$), what justifies the slight differences observed between graphs due to the method precision (e.g., AA in 1c and 1d).

Figs. 2 and 3 show the results that fit with the homogenous first and second order models.

According to the literature [8], the reaction between glycerol and acetic acid with 4:1 molar ratio (acetic acid/glycerol) follows a reversible second order model. By way of comparison, Fig. 4 was plotted, where the present experimental data received model fitting with a reversible second order model (4a) and irreversible first order model (4b). For the reversible second order model, the equilibrium constants from reference [8] were used: 5.45, 1.37 and 0.33 at $90 \text{ }^\circ\text{C}$, for reactions 4, 5 and 6.

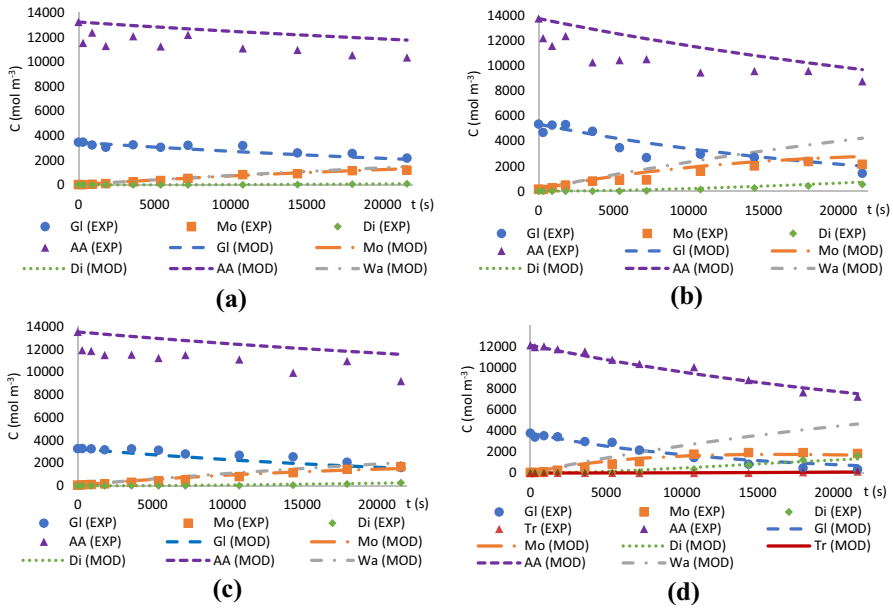


Fig. 1 MOD: Homogenous first order model and EXP: experimental data, the reaction was catalyzed by PS-TMPTA where **a** T580 is 5 g L^{-1} at $80 \text{ }^\circ\text{C}$; **b** T590 is 5 g L^{-1} at $90 \text{ }^\circ\text{C}$; **c** T1080 is 10 g L^{-1} at $80 \text{ }^\circ\text{C}$; **d** T1090 is 10 g L^{-1} at $90 \text{ }^\circ\text{C}$; *GI* glycerol, *Mo* monoacetin, *Di* diacetin, *Tr* triacetin; *AA* acetic acid; *Wa* water. Stirred speed is 350 rpm and molar ratio for acetic acid/glycerol is 4:1

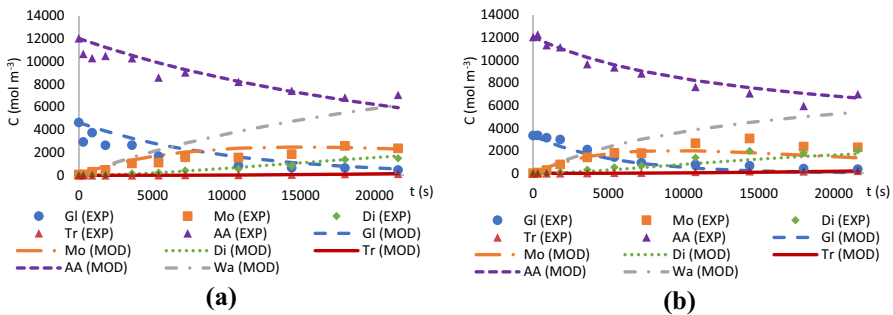


Fig. 2 MOD: Homogenous first order model and EXP: experimental data, the reaction was catalyzed by Amberlyst 36 where **a** A580 is 5 g L^{-1} at $80 \text{ }^\circ\text{C}$; **b** A590 is 5 g L^{-1} at $90 \text{ }^\circ\text{C}$; *GI* glycerol, *Mo* monoacetin, *Di* diacetin, *Tr* triacetin, *AA* acetic acid, *Wa* water. Stirred speed is 350 rpm and molar ratio for acetic acid/glycerol is 4:1

As can be seen, the fitting for both models are near identical as shown at Fig. 4. For the reversible second order model, the kinetic parameters were: $7.12 \pm 0.89 \times 10^{-9}$, $4.89 \pm 1.35 \times 10^{-9}$ and $7.39 \pm 1.43 \times 10^{-10} \text{ m}^3 \text{ mol}^{-1} \text{ s}^{-1}$ for k_1 , k_2 and k_3 , the P-values for these parameters were, in order: 0.00%, 0.07% and 60.83%, where the first one is null because it is below 10^{-6} ; and the AICc is 747.22. For the

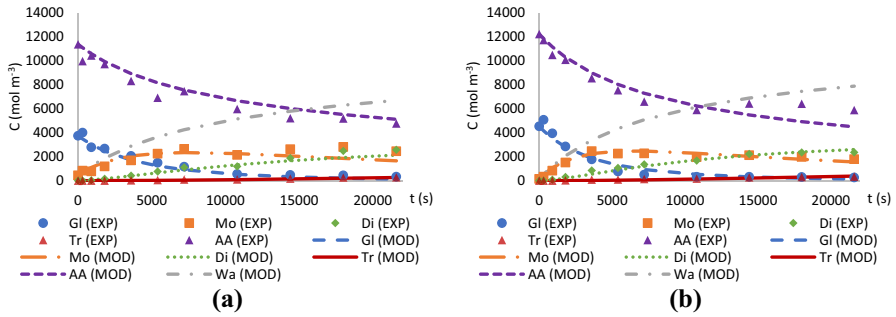


Fig. 3 MOD: Homogenous second order model and EXP: experimental data, the reaction was catalyzed by Amberlyst 36 where **a** A1080 is 10 g L^{-1} at $80 \text{ }^\circ\text{C}$; **b** A1090 is 10 g L^{-1} at $90 \text{ }^\circ\text{C}$; *GI* glycerol, *Mo* monoacetin, *Di* diacetin, *Tr* triacetin, *AA* acetic acid, *Wa* water. Stirred speed is 350 rpm and molar ratio for acetic acid/glycerol is 4:1

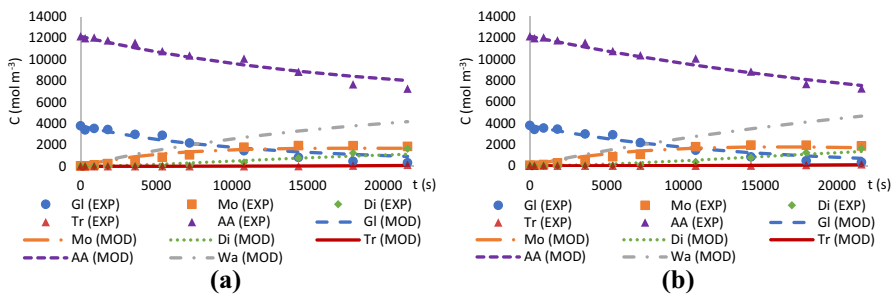


Fig. 4 The reaction was catalyzed by PS-TMPTA for T1090 (10 g L^{-1} and $90 \text{ }^\circ\text{C}$) where **a** MOD is reversible second order model; **b** MOD is irreversible first order model; *EXP* experimental data, *GI* glycerol, *Mo* monoacetin, *Di* diacetin, *Tr* triacetin, *AA* acetic acid, *Wa* water. Stirred speed is 350 rpm and molar ratio for acetic acid/glycerol is 4:1

P-value alone, it showed that the model is incapable to find a significant value for k_3 alone, since its result is above 5%. On the other hand, for the irreversible first order model, Table S1 shows P-values for k_1 , k_2 and k_3 : 0.00%, 0.00% and 0.80%; and its AICc is 720.86, which is 26.36 units lower than the reversible second order model and 20.15 units lower than the irreversible second order (Table S2). It can be stated that, for the range of experimental conditions used in the present work, the first order irreversible model was sufficient to represent the experimental data. Furthermore, the addition of parameters (equilibrium constants) by considering reversibility of the reactions did not improve the fitting results. It is likely that, for conditions where equilibrium plateaus are well defined for the concentration profiles (e.g., higher amounts of catalysts or higher reaction time), the reversible second order model may provide a better fitting.

Evaluating the Figs. 1 and 2, it can be observed that, even with a lower ion exchange capacity, the synthesized resin presented similar results in comparison with Amberlyst 36 (taking into account that IEC of Amberlyst 36 is more than three

times higher than IEC of PS-TMPTA). In Fig. 1b (T590) the acetic acid consumed was approximately 4 mol m^{-3} while Fig. 2b (A590, the same conditions but with commercial resin) the acetic acid consumed was almost 5 mol m^{-3} . In order to confirm the improved catalytic activity of the synthesized resin over the commercial one, the specific rate constant per unit of catalytic site (k_1') was calculated for both resins as follows.

$$k_1' = \frac{k_1}{\text{IEC} * C_{\text{cat}}} \quad (22)$$

here k_1 is the first order rate constant (s^{-1}), IEC is the ion exchange capacity (mol g^{-1}), C_{cat} is the catalyst's concentration (g m^{-3}) and k_1' is the specific rate constant per unit of catalytic site. The synthesized resin presented k_1' of $5.273 \times 10^{-6} \text{ m}^3 \text{ s}^{-1} \text{ mol}^{-1}$ while commercial resin presented $4.089 \times 10^{-6} \text{ m}^3 \text{ s}^{-1} \text{ mol}^{-1}$. These values of k_1' indicates that the efficiency per catalytic site of the synthesized resin is apparently higher in comparison with the commercial resin. Conversely, this difference in k_1' data can be better explained by attributing different sites accessibilities to the resins in function of their crosslinker lengths. Since the IEC of Amberlyst 36 is more than three times higher (5.45 mmol g^{-1}) than that of PS-TMPTA (1.50 mmol g^{-1}), the performance of Amberlyst 36 was better (Fig. S1), despite its k_1' value being lower. Anyway, it is evidenced the potential of PS-TMPTA to catalyze the present reaction with relatively small amount of catalytic sites, accounting that its swelling index presented an attractive value ($Sw=7$), which corroborates the explanation of an improved accessibility to catalytic sites.

Conclusion

It can be concluded that the synthesized resin cross-linked with TMPTA had better efficiency per catalytic site in comparison with Amberlyst 36 for the glycerol acetylation under the studied conditions. This behavior was explained by attributing a better accessibility to catalytic sites of the synthesized resin in comparison with Amberlyst 36, which is corroborated by the significantly different swelling indexes.

The kinetic modeling revealed that the reversibility was not relevant for the simulation of the cases studied herein. Thus, it can be concluded that simpler first order kinetic models can be used without impairing accuracy. The AICc also indicates that 8 from the 10 experiments fitted the irreversible first order model, including both catalyzed and blank experiments. The irreversible second order model provided better predictions than the first order model only for Amberlyst 36 at both 80 and 90 °C and 10 g L^{-1} of catalyst concentration. The kinetic parameters displayed accuracy, especially when compared to previous works.

Another important finding was the calculated catalytic efficiency, which was 230.122 for the synthesized resin (PS-TMPTA) compared to the commercial resin (64.762) Amberlyst 36, indicating a better performance of the synthesized resin, since both catalysts have the same catalytic sites. To confirm this general behavior presented for PS-TMPTA in the catalysis, the specific rate constant per unit

of catalytic site (k_1') was calculated for both resins (synthesized and commercial resin), with the synthesized resin showing a better performance, which was corroborated by the swelling index ($sw=7$), catalytic efficiency (230.122) and their lower ion exchange capacity (1.5 mmol g^{-1}).

Supplementary Information The online version contains supplementary material available at <https://doi.org/10.1007/s11144-021-02141-2>.

Acknowledgements The authors would like to thank FAPESP (Grant N^o 2017/26985-4) for the financial support.

References

1. Galan MI, Bonet J, Sire R et al (2009) From residual to useful oil: revalorization of glycerine from the biodiesel synthesis. *Bioresour Technol* 100(15):3775–3778. <https://doi.org/10.1016/j.biortech.2009.01.066>
2. Simasatitkula L, Arpornwichanop A (2019) Feasibility study of using waste cooking oil and byproduct from palm oil refinery for green diesel production. *Chem Eng Trans*. <https://doi.org/10.3303/CET1974001>
3. Okoye PU, Abdullah AZ, Hameed BH (2017) Synthesis of oxygenated fuel additives via glycerol esterification with acetic acid over bio-derived carbon catalyst. *Fuel* 209:538–544. <https://doi.org/10.1016/j.fuel.2017.08.024>
4. Tran TTV, Obpirompoo M, Kongparakul S et al (2020) Glycerol valorization through production of di-glyceryl butyl ether with sulfonic acid functionalized KIT-6 catalyst. *Carbon Resour Convers* 3:182–189. <https://doi.org/10.1016/j.crcon.2020.12.003>
5. Liao X, Zhu Y, Wang SG et al (2009) Producing triacetyl glycerol with glycerol by two steps: esterification and acetylation. *Fuel Process Technol* 90(7–8):988–993. <https://doi.org/10.1016/j.fuproc.2009.03.015>
6. Setyaningsih L, Siddiq F, Pramezy A (2018) Esterification of glycerol with acetic acid over Lewatit catalyst. *MATEC Web Conf* 154:01028. <https://doi.org/10.1051/mateconf/201815401028>
7. Zhou L, Nguyen TH (2012) Adesina AA (2012) The acetylation of glycerol over amberlyst-15: kinetic and product distribution. *Fuel Process Technol* 104:310–318. <https://doi.org/10.1016/j.fuproc.2012.06.001>
8. Banu I, Bumbac G, Bombos D et al (2020) Glycerol acetylation with acetic acid over Purolite CT-275. Product yields and process kinetics. *Renew Energy* 148:548–557. <https://doi.org/10.1016/j.renene.2019.10.060>
9. Carpegiani JA, Godoy WM, Guimarães DHP, Aguiar LG (2020) Glycerol acetylation catalyzed by an acidic styrene-co-dimethacrylate resin: experiments and kinetic modeling. *React Kinet Mech Cat* 130:447–461. <https://doi.org/10.1007/s11144-020-01788-7>
10. Mekala M, Thamida SK (2013) Goli VL (2013) Pore diffusion model to predict the kinetics of heterogeneous catalytic esterification of acetic acid and methanol. *Chem Eng Sci* 104:565–573. <https://doi.org/10.1016/j.ces.2013.09.039>
11. Godoy WM, Castro G, Nápolis L, Carpegiani JA et al (2020) Synthesis of sulfonated Poly[Styrene-co-(Trimethylolpropane Triacrylate)] and application in the catalysis of glycerol acetylation. *Macromol Symp* 394(1):1900169. <https://doi.org/10.1002/masy.201900169>
12. Penariol JL, Theodoro TR, Dias JR et al (2019) application of a sulfonated styrene–(Ethylene Glycol Dimethacrylate) resin as catalyst. *Kinet Catal* 60(5):650–653. <https://doi.org/10.1134/S0023158419050057>
13. Silva VFL, Penariol JL, Dias JR et al (2019) Sulfonated Styrene-Dimethacrylate resins with improved catalytic activity. *Kinet Catal* 60(5):654–660. <https://doi.org/10.1134/S0023158419050112>
14. Gomes FM, Pereira FM, Silva A (2019) Multiple response optimization: analysis of genetic programming for symbolic regression and assessment of desirability functions. *Knowl-Based Syst* 179:21–33. <https://doi.org/10.1016/j.knsys.2019.05.002>

15. Mufrodi Z, Rochmadi S, Budiman A (2012) Chemical kinetics for synthesis of triacetin from bio-diesel byproduct. *Int J Chem* 4(2):101–107. <https://doi.org/10.5539/ijc.v4n2p101>
16. Aguiar L, Moura JOV, Theodoro TR (2017) Prediction of resin textural properties by vinyl/divinyl copolymerization modeling. *Polymer* 129:21–31. <https://doi.org/10.1016/j.polymer.2017.09.042>
17. Coutinho FMB, Rezende SM (2006) Soares BG (2006) Characterization of sulfonated poly (styrene-divinylbenzene) and poly(divinylbenzene) and its application as catalysts in esterification reaction. *J Appl Polym Sci* 102(4):3616–3627. <https://doi.org/10.1002/app.24046>
18. Kunin R (1972) *Ion Exchange Resins*. Robert E Krieger Publ Co, New York
19. Theodoro TR, Moura JOV, Dias JR et al (2021) Mathematical modeling of Poly[styrene-co(ethylene glycol dimethacrylate)] sulfonation. *Kinet Catal* 62(1):188–195. <https://doi.org/10.1134/S0023158421010092>
20. Ferreira P, Fonseca IM, Ramos AM (2009) Esterification of glycerol with acetic acid over dodecamolybdophosphoric acid encaged in USY zeolite. *Catal Commun* 10(5):481–484. <https://doi.org/10.1016/j.catcom.2008.10.015>
21. Fogler HS (2006) *Elements of chemical reaction engineering*, 4th edn. Prentice Hall PTR, Upper Saddle River
22. Luenberger DG, Ye Y (2016) *Linear and nonlinear programming*, 4th edn. Springer International Publishing, New Jersey
23. Montgomery D, Runger GC (2018) *Applied statistics and probability for engineers*, 7th edn. Wiley, Hoboken
24. Aguiar LG, Godoy WM, Nápolis L et al (2021) Modeling the effect of cross-link density on resins catalytic activities. *Ind Eng Chem Res* 60(17):6101–6110. <https://doi.org/10.1021/acs.iecr.1c0095>
25. Moreira MN, Corrêa I, Ribeiro AM et al (2020) Solketal production in a fixed bed adsorptive reactor through the ketalization of glycerol. *Ind Eng Chem Res* 59(7):2805–2816. <https://doi.org/10.1021/acs.iecr.9b06547>

Publisher's Note Springer Nature remains neutral with regard to jurisdictional claims in published maps and institutional affiliations.